Available online at www.sciencedirect.com
ScienceDirect
Thermochimica Acta 453 (2007) 31–41
thermochimica acta
www.elsevier.com/locate/tca

Calibration of a quenching and deformation differential dilatometer upon heating and cooling: Thermal expansion of Fe and Fe–Ni alloys

G. Mohapatra, F. Sommer *, E.J. Mittemeijer

Max Planck Institute for Metals Research, Heisenbergstr. 3, D-70569 Stuttgart, Germany

Received 11 July 2006; received in revised form 2 November 2006; accepted 12 November 2006
Available online 17 November 2006

Abstract

Dilatometry is a technique for precise measurement of thermal dilatation of materials during heating or cooling. A procedure has been presented for calibration of a differential dilatometer operating with electromagnetic heating for metallic specimens both upon heating and cooling as well as under uniaxial compressive and tensile loading. The dilation signal has been calibrated for both heating and cooling and for uniaxial loading (compressive and tensile) using platinum or iron reference specimens, for which recommended dilational data are available. The ferro- to paramagnetic transition (characterised by the Curie temperature) of pure iron or iron-based alloys has been adopted to calibrate the temperature in the dilatometric measurement under different loading modes during heating and cooling. On this basis calibrated data for the thermal expansion coefficients of Fe and Fe–Ni alloys have been obtained.

Keywords: Dilatometer; Induction heating; Calibration; Heating; Cooling; Length change; Curie temperature

1. Introduction

Many solid materials exhibit structural changes, e.g. phase transformations, upon changing the temperature. These phase transformations are usually accompanied by a significant change in specific volume. The change in volume of a solid material is usually measured by the corresponding change in length of a specimen (long in one dimension) of this material. Thus, measurements of the change in length of solid materials are often applied for the determination of the kinetics of phase transformation of metals and alloys (e.g. [1–6]). Length-change measurement under applied compressive or tensile load during phase transformation makes it possible to investigate the influence of applied load on the phase transformation. If, upon increasing or decreasing the temperature, a phase transformation does not occur, the length of the specimen changes by thermal dilatation only, characterised by the linear thermal expansion coefficient, i.e., the relative length-change divided by the corresponding temperature interval.

The two principal factors that limit the accuracy of determination of the length-change by differential dilatometers are: (i) the thermal dilatation behaviour of the push-rods, which support the specimen and transmit the dilation signal, and (ii) the accuracy of the temperature determination of the specimen, because of the existing temperature gradient along the specimen-length axis due to heat loss by heat conduction from the specimen through pushrods and by radiation. Recently, a calibration procedure for the dilation and temperature signals upon heating and cooling in a differential dilatometer, provided with a resistance heated furnace, was proposed by Liu et al. [7]. In the present work the focus is on the use of a differential dilatometer operating with electromagnetic heating in the temperature range of about 300–1800 K applied to a solid, cylindrical, metallic specimen.

The construction and working principle of the dilatometer in the different modes (normal, compressive and tensile) have been briefly discussed in Section 2. Section 3 is dedicated to temperature profile measurement in the dilatometer specimen subjected to a heat treatment cycle. The calibration of the length-change as well of the temperature has been discussed in Section 4. The length-change calibrations for the normal (zero load) and compressive modes and for the tensile mode have been performed by taking pure Pt and pure Fe as reference specimens, respectively.

* Corresponding author. Tel.: +49 711 6893316; fax: +49 711 6893312.
E-mail address: f.sommer@mf.mpg.de (F. Sommer).

0040-6031/$ – see front matter © 2006 Elsevier B.V. All rights reserved.
doi:10.1016/j.tca.2006.11.007

The Curie temperature of pure Fe or Fe-based alloys has been taken as a standard for the absolute temperature calibration during heating and cooling experiments. Finally, Section 5 presents the linear thermal expansion coefficient (LTEC) data as determined in this work for pure Fe and Fe–Ni alloys.

2. Experimental

2.1. Dilatometer

The dilatometer used in this work (DIL-805A/D (A: quenching; D: deformation) dilatometer; Baehr-Thermoanalyse GmbH; cf. Fig. 1a–c) measures the specimen dilation as a function of temperature in the absence of a reference specimen. It is a differential dilatometer because two pushrods are used to measure the thermal dilation behaviour. The dilatometer can be used in normal (zero load) mode and deformation (uniaxial compressive/tensile) mode (see Fig. 1(a)–(c)). The electrically conductive specimen is heated inductively applying a water cooled induction Cu heating coil to generate a high frequency current. An additional inner Cu coil is perforated and thus can be used for inert gas quenching. The temperature of the specimen is controlled and measured with Pt–$Pt_{90}Rh_{10}$ thermocouples (type-s) spot welded on the specimen surface. The pushrods, used to transmit thermal dilation of the specimen and to also hold the specimen in normal (zero load) mode (cf. Fig. 1(a)), are either made of fused silica or alumina. The thermal dilation is measured via a linear variable differential transformer (LVDT) positioned in the measuring head. The whole system is insensitive to mechanical vibration. The LVDT and the specimen are kept isolated from each other by a dividing wall and hence the LVDT is not influenced by heat radiation or heat conduction from the specimen. The length-change resolution achievable with this instrument is about 50 nm.

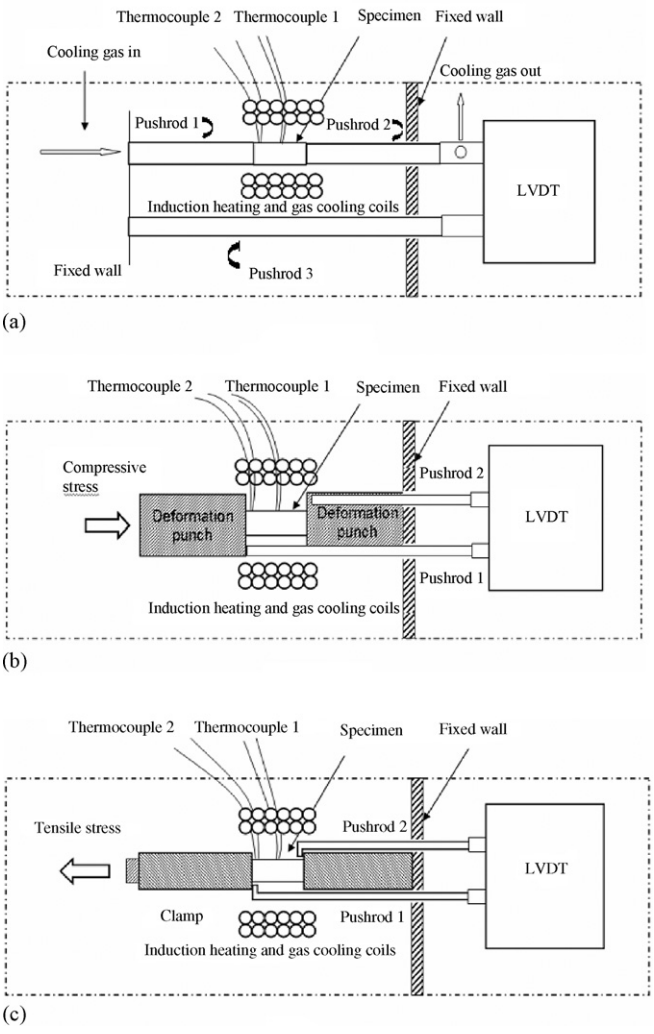

Fig. 1. Schematic (cross sectional top view) diagram showing the quenching and deformation differential dilatometer (from Baehr-Thermoanalyse GmbH) in different modes (a) normal mode (zero load mode), (b) compressive mode, and (c) tensile mode.

2.1.1. Normal mode

The normal mode of operation is schematically shown in Fig. 1(a). The pushrods 2 and 3 are connected to the LVDT. The specimen is supported by pushrods 1 and 2. Pushrod 1 is fixed at the left side of the specimen; pushrod 2 is fixed at the right side of the specimen and transmits the occurring dilation; pushrod 3 serves as reference. The specimen is a solid (or hollow) cylinder; typical specimen dimensions are length of 10 mm; diameter of 5 mm; wall thickness of 1 mm for a hollow specimen. The specimen can be heated inductively under vacuum to a defined temperature with a maximum allowable heating rate of 4000 K min^{-1} (upper limit of DIL-805A/D) and, for a solid specimen, can be continuously cooled applying a cooling rate of maximal 200 K min^{-1} and, with additional Ar flow through the inner, perforated Cu coil, applying a cooling rate of maximal about 1600 K min^{-1}. Ar gas can be led additionally through a hollow specimen to achieve large cooling rates up to 2500 K min^{-1}.

2.1.2. Compressive mode

The compressive mode of operation is schematically shown in Fig. 1(b). Pushrods 1 and 2 are connected to the LVDT. The specimen is supported at both sides by deformation punches. The specimen dilation is transferred via pushrod 1; pushrod 2 serves as reference. The specimen can be deformed (elastically/plastically) during heat treatment under simultaneous recording of length-change. Deformation punches are made of fused silica or alumina and have a diameter of 12 mm and a length of 35 mm. The left punch is used to apply the uniaxial, compressive load, whereas the other punch is fixed. The load, generated by a hydraulic system, is transferred via a hydraulic cylinder. The maximum applied load is limited to 25.0 kN with a sensitivity of ±0.0005 kN. The accessible heating and cooling rates in this mode are in the range or 2500 and 200 K min^{-1}, respectively.

2.1.3. Tensile mode

The tensile mode of operation is schematically shown in Fig. 1(c). The specimen to be used in the tensile mode has a geometry different from that used in the normal or compressive modes. The solid, cylindrical specimen has a central part

Table 1
Chemical composition of the iron and nickel used

Element	Fe	Ni
C	11	23
Si	13	0.23
Cu	1	0.18
Ti	0.6	5.3

Unit: ppm in mass.

of length 10 mm and of diameter 5 mm, as in the normal and compressive modes, but now incorporates two additional parts (clamps) at both sides of length 29.5 mm and of diameter 9 mm. This relatively long specimen is screwed on the wall at the right side; the uniaxial tensile load is applied at the left side. The pushrods transmitting the dilation of the specimen to the LVDT are positioned in contact with the specimen as shown in Fig. 1(c): pushrod 1 measures the dilation of the specimen relative to pushrod 2.

2.2. Alloy preparation

As model systems pure Fe and Fe–Ni alloys were chosen. Iron was supplied by Aldrich GmbH and nickel was supplied by Alfa Aesar GmbH; for compositions, see Table 1. The as-received pure Fe rods were hammered down to rods with a diameter of about 6 mm, for both normal and compressive mode specimens. Fe–Ni alloys were prepared by melting appropriate amounts of Fe and Ni in a vacuum arc melting furnace; the molten alloy was cast in a copper mould of 7 mm diameter. The as cast ingots were hammered down to rods of 6 mm diameter, for both normal and compressive mode specimens. To prepare tensile mode specimens, castings of pure Fe, of dimensions 100 mm length and 10 mm diameter, were made and subsequently hammered down to rods of 9.5 mm diameter.

In order to achieve a homogeneous microstructure, all the rods/castings were sealed in a quartz container filled with argon gas at 2×10^4 Pa. The specimens were heated from room temperature to 1423 K at 5 K min^{-1} followed by annealing at 1423 K for 100 h and subsequently furnace cooled to room temperature. Thereafter the compositions of the Fe–Ni rods were determined by inductive coupled plasma-optical emission spectrometry (ICP-OES). The composition of the Fe–Ni alloys used was found to be: Fe–2.96 at.%Ni and Fe–5.93 at.%Ni.

Next, to prepare normal and compressive mode specimens, the rods were machined to dilatometry specimens with a diameter of 5 mm and a length of 10 mm. To prepare tensile mode specimens the rods were machined to dimensions as shown in Fig. 1(c) and discussed in Section 2.1.3.

3. Temperature measurement

Dilatometry specimens undergoing an inductive heating and cooling cycle experience a temperature inhomogeneity during heating and cooling. The temperature inhomogeneity is largely attributed to heat loss by heat conduction through the material (pushrods, deformation punches and clamps) holding the specimen (cf. Fig. 1a–c); heat loss by radiation is largely compensated by additional heating induced by the temperature read out by thermocouple 1 (Fig. 1(a)) controlling the inductive heating.

3.1. Temperature profile measurement

The temperature of the specimen during heating and cooling is controlled and measured with $Pt_{90}Rh_{10}$–Pt thermocouples (S-type) spot welded on the specimen surface.

The locations of the spot welded thermocouples to implement the programmed temperature and to measure the temperature profile during heat treatment are schematically shown in Fig. 1(a)–(c). Thermocouple 1 is spot welded at the centre of the specimen to control the temperature according to the chosen temperature program. Thermocouple 2 is spot welded at the extreme end of the specimen to measure the temperature at one end of the specimen and thus assess the temperature gradient in the specimen.

The temperatures measured with thermocouple 1 (T_{centre}) and thermocouple 2 (T_{end}) at a program temperature of 923 K for two different Fe–5.93 at.%Ni specimens subjected to 20 K min^{-1} heating and cooling are shown in Table 2 for normal, compressive and tensile modes. The temperature gradient in both specimens is not the same for the same heating and cooling cycle which is due to the lack of reproducibility in spot welding of thermocouples or differences in the surface contacts between the pushrods (or punches) and the specimen or differences in the position of the specimen inside the induction coil. A correction procedure has been developed and has been presented

Table 2
Measured temperatures T_{centre} and T_{end} for a set program temperature of 923.0 K (i.e. before the start temperature of the $\gamma \rightarrow \alpha$ transformation upon cooling for Fe–5.93 at.%Ni) for two different specimens each with a heating and cooling rate of 20 K min^{-1} for normal, compressive and tensile modes

Mode	Specimen	Heating			Cooling		
		T_{centre} (K)	T_{end} (K)	$\Delta T_{heating}$	T_{centre} (K)	T_{end} (K)	$\Delta T_{cooling}$
Normal	1	923.0	919.2	3.8	923.0	915.9	7.1
	2	923.0	918.2	4.8	923.0	916.1	6.3
Compressive	1	923.0	919.7	3.3	923.0	918.0	5.0
	2	923.0	920.1	2.9	923.0	916.3	4.7
Tensile	1	923.0	922.2	0.8	923.0	921.9	1.1
	2	923.0	922.5	0.5	923.0	922.2	0.8

elsewhere [8] that enables full correction for the temperature inhomogeneity and as a result the length-change as a function of a homogeneous temperature can be presented. This procedure has been adopted in this paper if the gradient ($T_{centre} - T_{end}$) in the specimen was larger than 1.0 K.

4. Calibration procedures

4.1. Introductory remarks

Calibration of the dilation upon heating and cooling is performed, for the normal and compressive modes, by measuring the length-change of a cylindrical Pt reference specimen with diameter of 2.99 mm and length of 10.04 mm and, for the tensile mode, by measuring the length-change of a Fe reference specimen of pure Fe (large overall specimen size). The difference between the measured $\Delta L/L_0$ for the reference specimens and the recommended (reference) values for the dilatation of the platinum or iron specimen upon heating and cooling serves as a calibration (additive correction) for the relative length-change ($\Delta L/L_0$) values recorded in measurement runs performed with specimens to be investigated applying the same heat treatment procedure. The extent of the corrections depends upon temperature program employed (heating/cooling rates, see Table 3) and type of pushrods used (alumina or fused silica (see Fig. 2)), recognizing the different thermal conductivities of the different types of pushrods. To demonstrate the consequences of the choice of the type of pushrods, two heat treatment cycles were performed in normal mode, with a heating and cooling rate of 20 K min^{-1} and an intermediate isothermal holding for 30 min at 1273 K, for the Pt reference specimen, the first time with the alumina pushrods and the second time with the silica pushrods. The difference in the $\Delta L/L_0$ values for the heating and cooling parts of the heat treatment cycle is much larger for using the alumina pushrods than for using the silica pushrods. This can be understood as a consequence of the fused silica having a lower thermal conductivity [9] and lower thermal expansion [9] than the alumina (LTEC of silica and alumina are around 0.5×10^{-5} and 1.0×10^{-5} K^{-1}, respectively).

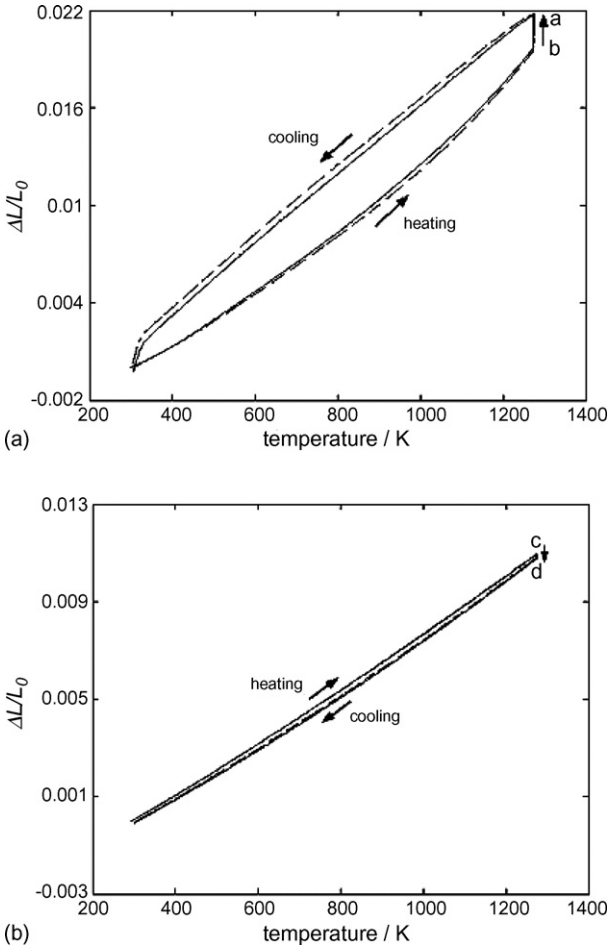

Fig. 2. Measured length-change in normal mode as a function of temperature of the Pt reference specimen for two successive cycles during constant heating (20 K min^{-1}) from room temperature to 1273 K and subsequent cooling (20 K min^{-1}) interrupted by an isothermal annealing at 1273 K for 30 min: (a) alumina pushrods; (b) fused silica pushrods.

An increase of the relative dilation of the specimen occurs during isothermal holding at 1273 K for using alumina pushrods (shown by b ⇒ a in Fig. 2(a)). This can be understood as follows. The alumina pushrods have a relatively high thermal conductiv-

Table 3
Measured average Curie temperature (for two cycles), $T_{C,meas}$ characterising the ferro- to paramagnetic transition, the temperature shift (calibration correction), ΔT_C (=$T_C - T_{C,meas}$) (T_C = 1043 K [12]) as given by the difference of the reference value of the Curie temperature and the measured value

Rates (K min^{-1})	Heating		Cooling	
	$T_{C,meas}$ (K)	ΔT_C (K)	$T_{C,meas}$ (K)	ΔT_C (K)
10	1035.3 ± 0.5	7.7	1034.8 ± 0.5	8.2
20[a]	1035.8 ± 2.1[a]	7.1	1034.9 ± 2.5[a]	8.1
50	1036.4 ± 0.5	6.6	1034.6 ± 0.4	8.4
100	1036.2 ± 0.6	6.9	1033.3 ± 0.8	9.7
150	1036.4 ± 0.5	6.6	1031.3 ± 1.0	11.7
200	1036.6 ± 0.5	6.4	1027.7 ± 1.1	15.3
300	1036.2 ± 1.2	6.8	[b]	[b]
400	1037.5 ± 1.0	5.4	[b]	[b]
500	1037.8 ± 1.4	5.2	[b]	[b]

[a] The average Curie temperature for a repeated set of 25 experiments with a heating and cooling rate of 20 K min^{-1}.
[b] The Curie temperature could not be detected precisely from the drop in expansion coefficient (see Fig. 5) as a function of measured temperature, because at high cooling rates (200 K min^{-1} and above) the drop in linear expansion coefficient is within the scatter of the measured LTEC data.

ity and, after heating up, upon subsequent isothermal holding at 1273 K the pushrods need time to reach thermal equilibrium. Hence, the pushrods (pushrods 1 and 2 in Fig. 1(a)) continue to expand at the isothermal holding temperature. This results in a virtual increase in relative dilation (b ⇒ a) of the specimen during the isothermal holding at 1273 K (see Fig. 2(a)). A reverse phenomenon, i.e. a small decrease in relative dilation upon isothermal holding at 1273 K (shown by c ⇒ d in Fig. 2(b)), occurs for using fused silica pushrods. This can be understood as follows. As a consequence of radiative heat transfer from the specimen to its surroundings the reference pushrod 3 (see Fig. 1(a)) expands relative to pushrods 1 and 2 and this results in a small decrease in relative dilation. The temperature of the reference pushrod 3 was measured additionally during the heat treatment cycle. Indeed, the measured temperature of pushrod 3 after 30 min of isothermal holding at 1273 K had increased with about 24 K. If the thermal expansion coefficient of fused silica is taken as $0.5 \times 10^{-5}\,K^{-1}$ [9] then the increase in relative length-change ($\Delta L/L_0$) corresponding to an increase in temperature of 24 K is 12×10^{-5} which agrees well with the observed relative dilation as given by c ⇒ d which equals 10×10^{-5}. Further, the measured relative dilation and its temperature dependences (slopes in Fig. 2) are larger using the alumina pushrods than using the fused silica pushrods. This is ascribed to the thermal expansion coefficient of alumina being larger than that of fused silica and to the different temperature changes for the same heat treatment cycle due to different thermal conductivity in both types of the pushrods.

Calibration of temperature depends also on the heating and cooling rate employed. Hence, to each heating and cooling rate to be used, a separate temperature calibration has to be performed, or inter- or extrapolation of calibration parameters with respect to heating/cooling rate has to be performed.

It was recently proposed to adopt the Curie temperature corresponding to the ferro- to paramagnetic phase transformation in e.g. pure iron for temperature calibration upon heating and (also) upon cooling. This idea was successfully applied to the calibration of differential thermal analysis (DTA) for determining the heat capacity in heating and cooling experiments [10] and to the differential dilatometer to measure the specific volume change on heating and cooling, respectively [7].

4.2. Length-change calibration

4.2.1. Normal and compressive modes

The correction to the measured relative length-change of the specimen under investigation is a consequence of the (undesired) thermal dilation of the pushrods/deformation punches in thermal contact with the specimen surface. To determine the true relative length-change, a correction term should be added to the measured relative length-change for each temperature for any specimen to be investigated.

A polycrystalline, platinum dilatometric specimen, of the same geometry as the specimen to be investigated, serves as the reference specimen. Then the calibration or correction term $(\Delta L/L_0)_{cal,i}$ is given by the difference of the known true relative length-change of the reference specimen $(\Delta L/L_0)_{ref}$ [11] and the measured length-change for the reference specimen $(\Delta L/L_0)_{ref,meas,i}$:

$$\left(\frac{\Delta L}{L_0}\right)_{cal,i} = \left(\frac{\Delta L}{L_0}\right)_{ref} - \left(\frac{\Delta L}{L_0}\right)_{ref,meas,i} \quad (1)$$

where i, stands for either heating or cooling. Hence, the corrected length-change of the specimen to be investigated $(\Delta L/L_0)_i$ then is given by

$$\left(\frac{\Delta L}{L_0}\right)_{i} = \left(\frac{\Delta L}{L_0}\right)_{meas,i} + \left(\frac{\Delta L}{L_0}\right)_{cal,i} \quad (2)$$

where $(\Delta L/L_0)_{meas,i}$ is the measured length-change.

The measured length-change of the cylindrical platinum reference specimen upon heating and cooling is shown in Fig. 3, employing the fused-silica pushrods in normal mode (Fig. 3(a)) and the fused silica solid punches in compressive mode (Fig. 3(b)). The following isochronal heat treatment program was executed: the specimen was heated from room temperature up to 1273 K (at 20 K min^{-1}), kept at this temperature for 30 min, and then the specimen was cooled down continuously to 300 K (at 20 K min^{-1}). By subtracting the measured data from the known $(\Delta L/L_0)_{ref}$ values of the platinum, the corresponding calibration data $(\Delta L/L_0)_{cal}$ are obtained for heating and cooling, respectively (cf. Eq. (1)). As indicated in Section 4.1, the correction $(\Delta L/L_0)_{cal}$ is different for heating and cooling. Moreover a slight difference in correction, for both heating and cooling, occurs between the normal and compressive modes, reflecting the difference in dilatometric geometry (cf. Fig. 1(a) and (b)).

4.2.2. Tensile mode

A polycrystalline, iron dilatometric specimen of the same geometry as the specimen to be investigated, serves as the reference specimen. The reference, relative length-change of iron as a function of temperature has been obtained using the analytical expression for LTEC of the austenite and ferrite phases, as discussed in Section 5. The calibrated relative length-change is derived from the measured relative length-change following the same procedure as described in Section 4.2.1. The obtained calibrations in this mode, for the heat treatment cycle described in Section 4.2.1, are shown in Fig. 3(c). It should be recognised that, (1) the calibrations for heating and cooling are different, for both the α and γ phases, as also observed for the normal and compressive modes, and (2) the calibrations for the α and γ phases are different, exhibiting a sharp discontinuity at the α → γ and γ → α phase transformations.

The length change calibration during γ → α transformation was done as follows: first the transformed fraction f_α was determined from the measured length change adopting the lever rule [4]. Secondly, taking into account the f_α and extrapolated calibration length changes for the pure α and γ phases in the γ → α transformation range, the length change calibration during γ → α transformation is given by:

$$(\Delta L)_{cal,\gamma\to\alpha} = f_\alpha(\Delta L)_{cal,\alpha} + (1 - f_\alpha)(\Delta L)_{cal,\gamma} \quad (3)$$

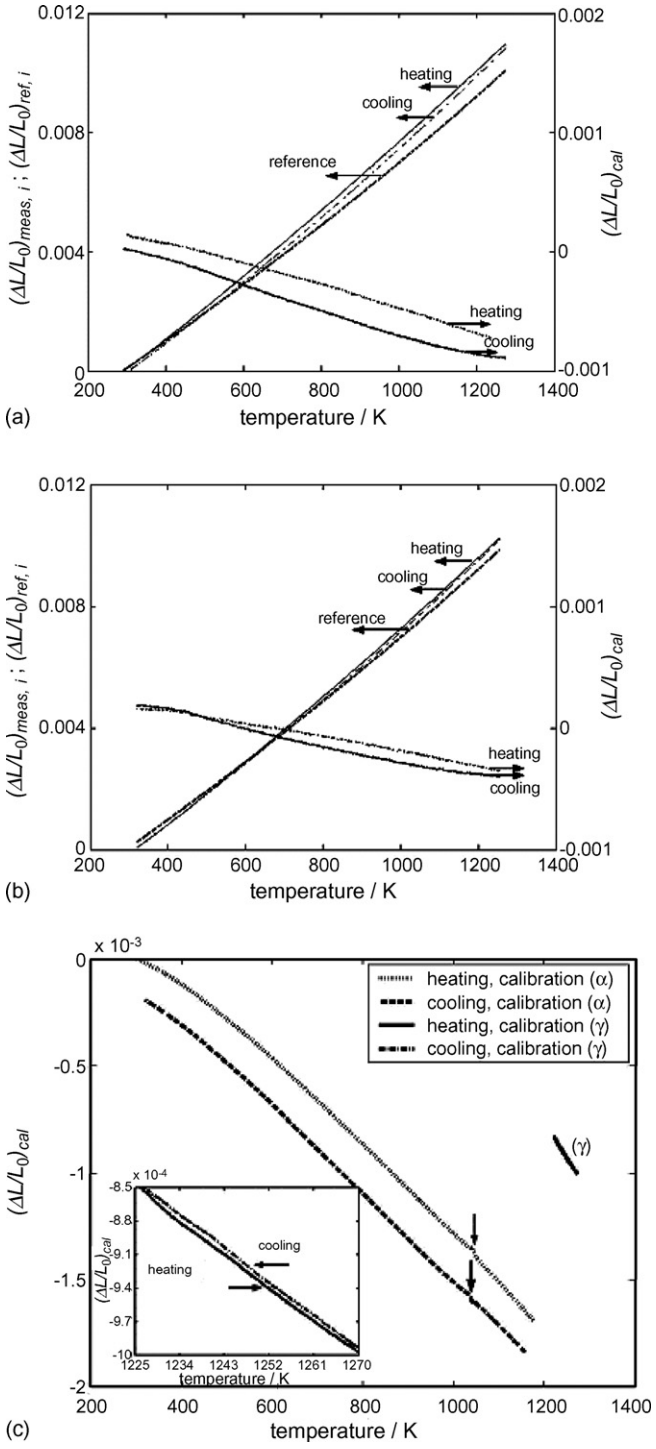

Fig. 3. The relative length-change, as measured for the Pt reference specimen $(\Delta L/L_0)_{meas}$, the corresponding data according to Ref. [12] and the resulting relative length scale corrections $(\Delta L/L_0)_{cal}$ (right ordinate in (a) and (b)) upon continuous heating (20 K min^{-1}) from room temperature to 1273 K and subsequent continuous cooling (20 K min^{-1}) interrupted by an isothermal annealing at 1273 K for 30 min, with fused silica pushrods: (a) normal mode, (b) compressive mode, and (c) the obtained $(\Delta L/L_0)_{cal}$ upon heating and cooling with a pure Fe specimen subjected to the aforementioned temperature program; tensile mode; the vertical arrows indicate the measured Curie temperature upon heating and cooling in the single ferrite (α) phase region; the inserted blow up shows $(\Delta L/L_0)_{cal}$ for the single austenite (γ) phase region shown as an apparently single line in the main figure.

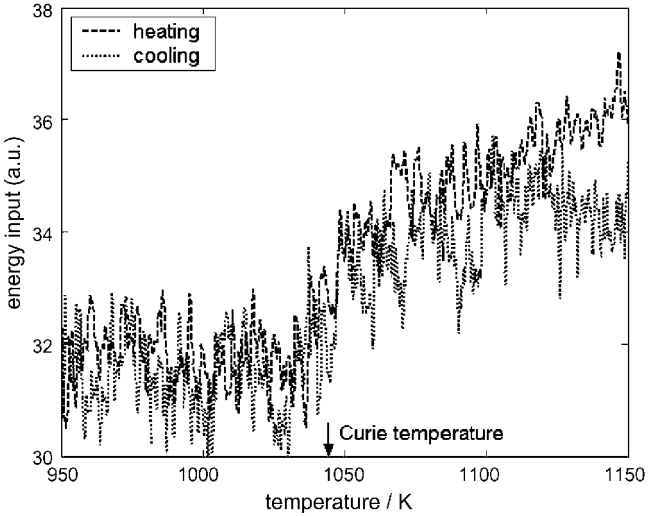

Fig. 4. Energy input as a function of temperature (T_{centre}) upon heating and cooling (with 20 K min^{-1}) for pure iron in the vicinity of the true Curie temperature (=1043 K [12]). The rise of energy input upon heating and the drop of energy input upon cooling indicate the measured Curie temperature during heating and cooling, respectively.

where $(\Delta L)_{cal,\alpha}$ and $(\Delta L)_{cal,\gamma}$ are the calibrated length changes for the pure α and γ phases, respectively (see Fig. 3(c)). A similar expression can also be given for length change calibration during $\alpha \rightarrow \gamma$ transformation.

4.3. Temperature calibration

Execution of the temperature calibration is independent of the mode of operating the differential dilatometer. As an example the calibration procedure is discussed here for the normal mode (cf. Fig. 1(a)). Several heat treatment cycles for different heating rates (10–500 K min^{-1}) and cooling rates (10–500 K min^{-1}) were performed with pure iron as the specimen. The occurrence of the ferromagnetic transition was exhibited by a hump on the length-change curve [cf. Fig. 9(b)] as well as by a perceivable rise/drop in energy input (cf. Fig. 4) for heating/cooling. Fig. 9(b) also shows a relative length-change curve upon heating indicating the magnetic transition and a blow up of the magnetic transition against an interpolated length change without magnetic transition. Because of the temperature ranges observed for the rise/drop in energy input and the hump in length-change during magnetic transition it is difficult to identify the temperature for magnetic transition. The LTEC of ferritic Fe as determined (according to Eq. (5) given in Section 5) from the dilatometer measurements at a heating and cooling rate of 20 K min^{-1} is shown in Fig. 5. The distinct minimum in the linear thermal expansion coefficient indicated with arrows in Fig. 5 represents the Curie temperature for heating and cooling.

Since the dilatometric specimen exhibits a temperature gradient, during heating and cooling, which is also not constant from one experiment to another (see Section 3.1), in principle the average of the measured temperatures T_{centre} and T_{end} (cf. Section 3) is used as the "measured" temperature of the specimen.

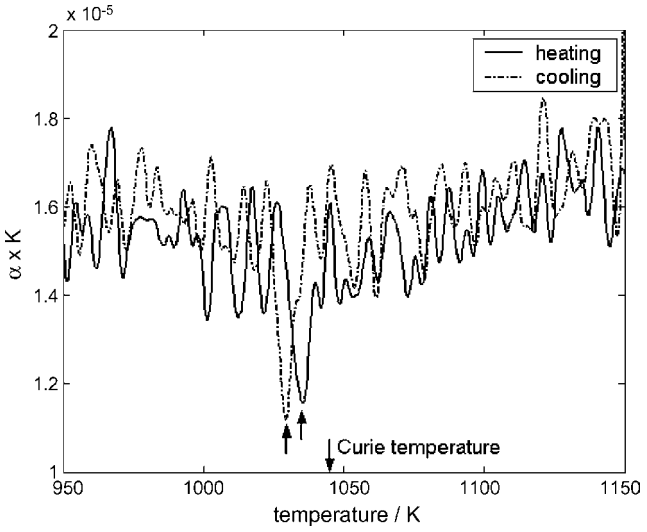

Fig. 5. Linear thermal expansion coefficient (α) of ferritic pure iron, as a function of temperature (T_{centre}), as determined from dilatometric measurements applying a heating and cooling rate of 20 K min^{-1}. The true Curie temperature [12] and the apparent Curie temperature have been indicated with arrows.

However, the enthalpy consumption by the magnetic transition poses a problem here, that is dealt with as follows.

The LTEC and the temperatures T_{centre} and T_{end} have been plotted as a function of time in Fig. 6. The temperature T_{centre} varies linearly where as T_{end} varies nonlinearly during the magnetic transition. The temperature T_{centre} changes linearly with time because the thermocouple 1 measuring the temperature T_{centre} compensates, by controlling the induction heating, a change in temperature in the centre of the specimen due to enthalpy consumption upon magnetic transition. This is not the

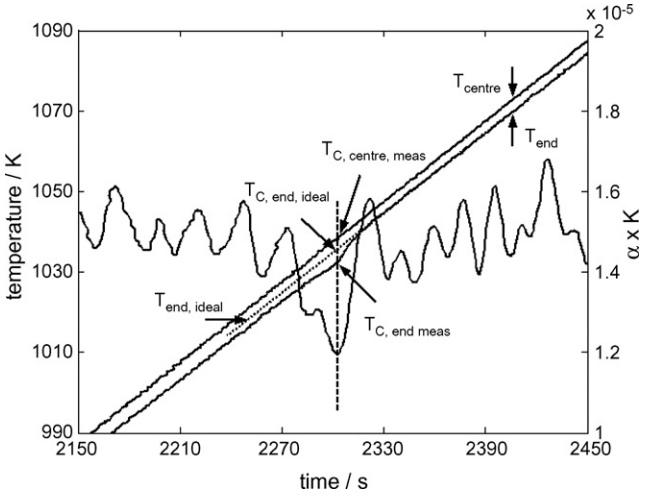

Fig. 6. The measured temperatures T_{centre} and T_{end} and linear thermal expansion coefficient (α) (showing a hump at the magnetic transition) as a function of time. $T_{end,ideal}$ (dashed line) is the interpolated temperature, which would have been the ideal temperature T_{end} in the absence of magnetic transition. The temperatures (T_{centre} and T_{end}) corresponding to the magnetic transition, as given by the intersection of the vertical dashed line at the magnetic transition (identified by the lowest value of α) with the temperature lines of T_{centre} and T_{end} are $T_{C,centre,meas}$ and $T_{C,end,meas}$, respectively. The intersection of the dashed vertical line with the temperature $T_{end,ideal}$ then gives the temperature $T_{C,end,ideal}$.

case for (especially) the ends of the specimen, where the temperature, T_{end}, has been measured by thermocouple 2. Hence, the temperature T_{end} does not change linearly with time during the transition: the drop observed in temperature T_{end} is due to the enthalpy change upon magnetic transition. In the ideal case, the temperature T_{end} that thermocouple 2 would have recorded, if no heat consumption due to the magnetic transition would occur (as is the case for a specimen to be investigated in this temperature range, in the absence of enthalpy change due to phase transformation), can be obtained by (linear) interpolation from the linear changes in T_{end} outside the temperature range where the minimum of the LTEC occurs; this temperature has been indicated with $T_{end,ideal}$ in Fig. 6. Thus, during the magnetic transition (i.e., at the Curie temperature, indicated by subscript C) the average measured temperature of the specimen is given by:

$$T_{C,meas} = \frac{T_{C,centre,meas} + T_{C,end,ideal}}{2} \quad (4)$$

where $T_{C,end,ideal}$ is the interpolated temperature T_{end} at the Curie temperature. The thus measured Curie point temperatures, $T_{C,meas}$ ($=T_{C,centre,mass} + T_{C,end,ideal}/2$) and the corresponding temperature corrections (ΔT_c), adopting the true Curie temperature of pure iron as reference (1043.0 K [12]), have been listed in Table 3, for a number of heating and cooling rates. For all the experiments pertaining to Table 3 the same specimen was used without taking it out from the dilatometer, ensuring there is no change in spot welding and the location of the specimen inside the coil, which changes might otherwise have led to a different temperature gradient in the specimen.

The obtained temperature corrections (shifts) ΔT_C, for the different heating and cooling rates, are shown in Fig. 7(a) and (b), respectively. In order to find out the variation in ΔT_C due to different specimen mountings in the dilatometer a set of experiments was performed for a heating/cooling rate of 20 K min^{-1}. For each experiment, a fresh specimen was taken and a fresh thermocouple spot welding was done. The results are represented by the distributions shown in Fig. 8. The average Curie temperature was obtained as 1036.5 ± 2.1 and 1035.3 ± 2.5 K upon heating (Fig. 8(a)) and cooling (Fig. 8(b)), respectively. The difference in measured Curie temperature between heating and cooling is about 1 K ($1036.5 \pm 2.1 - 1035.3 \pm 2.5$). The standard deviations in ΔT_C for heating and cooling at 20 K min^{-1} have also been indicated in Fig. 7.

5. Relative length-change calibration of pure Fe (normal, compressive and tensile modes)

The relative length change of pure iron, using the normal mode measured upon the heat treatment procedure indicated in Section 4.2.1, is shown in Fig. 9(a), before and after calibration of both the temperature and the length-change scales applying the methodology developed in Section 4. Similar relative length-change results (before and after calibration) are obtained using the compressive mode. The segment AB of the calibrated curve corresponds to the thermal expansion of the specimen upon continuous heating in the absence of a phase transforma-

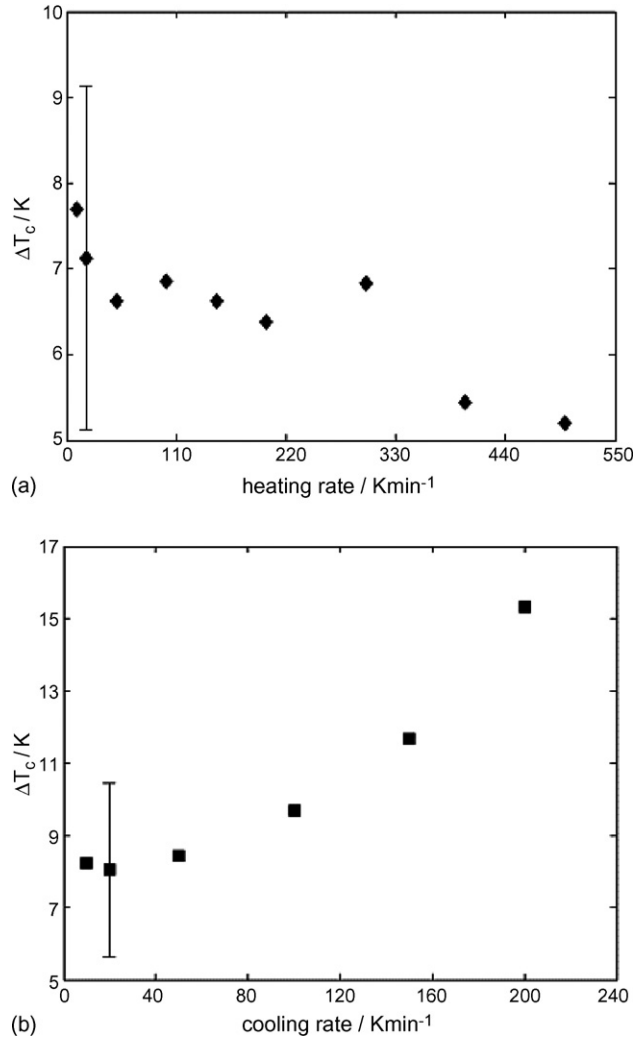

Fig. 7. Temperature scale correction, ΔT_C, for various heating rates (a) and cooling rates (b). A single specimen with the same pair of welded thermocouples was applied. The scatter in the temperature calibration for a repeated sets of experiments (number: 25) at 20 K min^{-1} heating and cooling with now for each experiment a freshly spot welded pair of thermocouples has been indicated too.

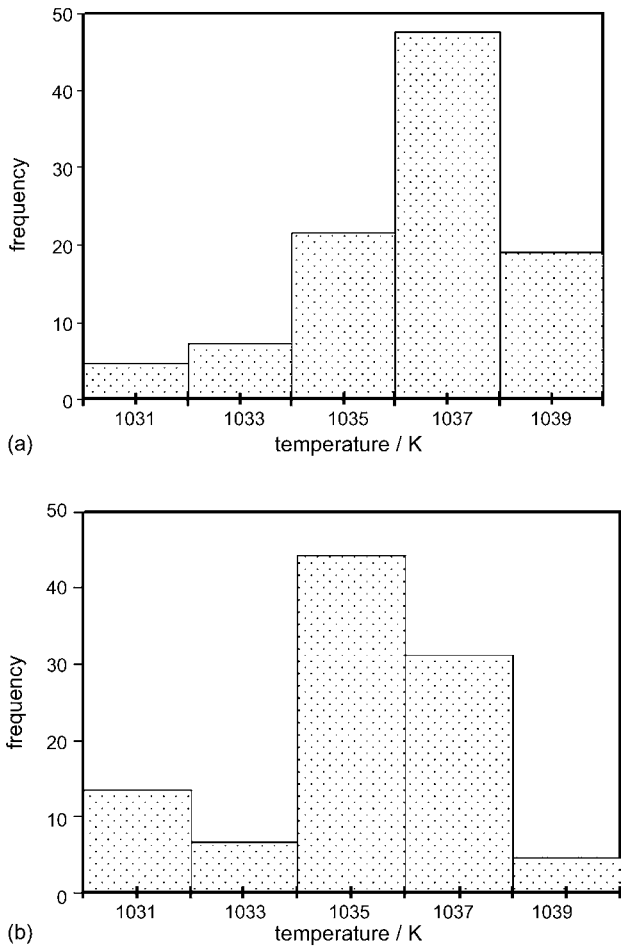

Fig. 8. The distribution of the values measured for the Curie temperature ($T_{C,meas}$) during heating (a) and cooling (b) for a heating and cooling rate of 20 K min^{-1} for repeated (number: 25) sets of experiments using for each experiment a freshly spot welded pair of thermocouples.

tion. Part BC represents the $\alpha \rightarrow \gamma$ transformation, during which a length contraction occurs due to the formation of austenite. Parts CD and EF stand for the expansion and contraction of austenite upon heating and subsequent cooling, respectively. Part FG corresponds to the $\gamma \rightarrow \alpha$ transformation, associated with length increase. After completion of the $\gamma \rightarrow \alpha$ transformation the length of the specimen decreases continuously down to room temperature due to thermal contraction (indicated by GH).

The measured relative length change of pure iron, using the tensile mode device without applying load, upon the heat treatment procedure indicated in Section 4.2.2, is shown in Fig. 10(a), before and after calibration of both the temperature and the length-change scales, applying the methodology developed in Section 4. As compared to the (linear) thermal expansion/shrinkage, a small rise in specimen length occurs at the end of $\alpha \rightarrow \gamma$ transformation and a small drop in specimen length occurs before the start of $\gamma \rightarrow \alpha$ transformation, according to the relative length-change data as a function of temperature (see Fig. 10 (b)). This effect is due to the prevailing temperature gradient in the specimen. The clamps are part of the entire specimen and therefore of the same material as the inner part of the specimen that is used for measuring the dilation (see Section 2.1.3; Fig. 1(c)) The portions of the clamps in contact with the pushrods (see Fig. 1(c)) are at a lower temperature than the inner part of the specimen because large parts of the clamps are outside the heating zone (i.e. outside induction coil) (cf. Fig. 1(c)). Hence, upon cooling they start to transform earlier than the inner part of the specimen. In that stage, then the pushrods 1 and 2 move towards each other (because of the transformation induced volume expansion) and thereby cause an apparent decrease in relative length-change just before the start of $\gamma \rightarrow \alpha$ transformation in the inner part of the specimen. A similar reasoning can be applied for the heating run and explain the apparent increase in relative length change at the end of the $\alpha \rightarrow \gamma$ transformation due to later completion of this transformation in the outer part (clamps) of the specimen. The start temperature of the $\gamma \rightarrow \alpha$ transformation and the end temperature of the $\alpha \rightarrow \gamma$ transformation are taken as the temperatures corresponding to the minimum of relative length-change (see the vertical arrows in Fig. 10(b)).

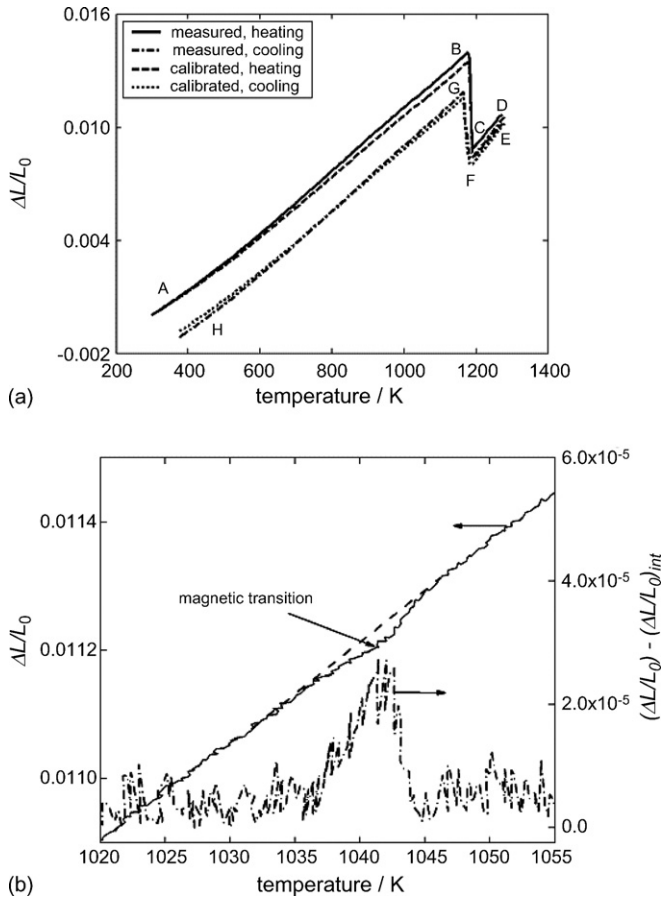

Fig. 9. (a) Comparison of the measured relative length-change as a function of temperature (T_{centre}) and corrected relative length-changes of pure iron (normal mode) during continuous heating (20 K min^{-1}) from room temperature to 1273 K and subsequent continuous cooling (20 K min^{-1}), interrupted by an isothermal annealing at 1227 K for 30 min. (b) The relative length-change curve upon heating indicating the magnetic transition and a blow up of the magnetic transition against an interpolated length change $(\Delta L/L_0)_{int}$, without magnetic transition.

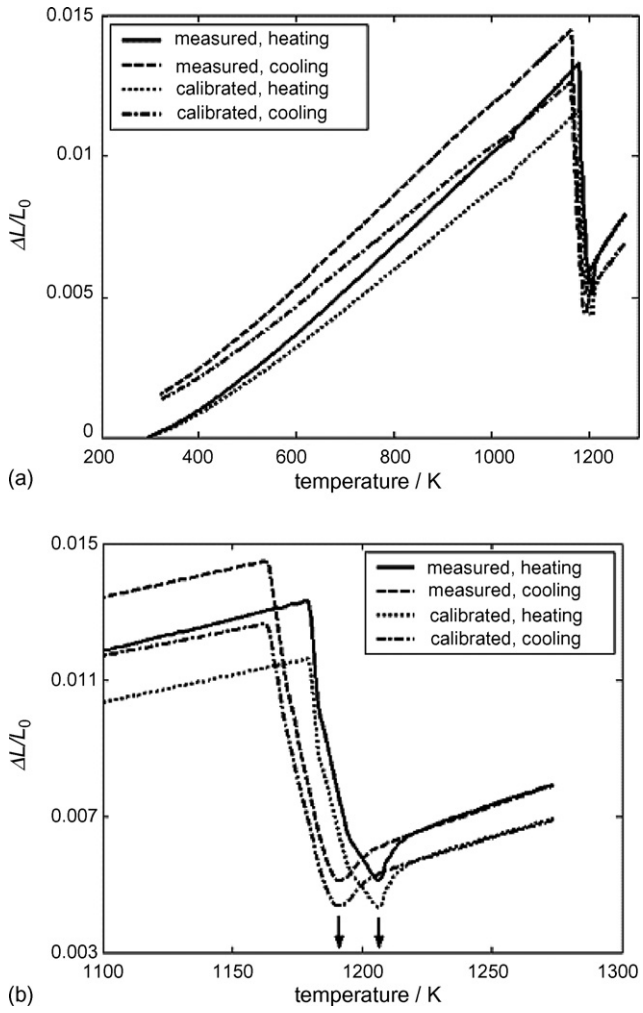

Fig. 10. (a) Comparison of the measured and corrected relative length-changes as a function of temperature (T_{centre}) of pure iron, using the tensile mode device without applying a load, upon continuous heating (20 K min^{-1}) from room temperature to 1273 K and subsequent continuous cooling (20 K min^{-1}), interrupted by an isothermal annealing at 1273 K for 30 min. (b) Enlargement of the measured length-change during heating and cooling in Fig. 10(a) indicating the sudden rise (heating) and fall (cooling) in measured relative length-change. The vertical dashed arrows indicate the measured end temperature of the $\alpha \rightarrow \gamma$ transformation and start temperature of the $\gamma \rightarrow \alpha$ transformation upon heating and cooling, respectively.

6. Linear thermal expansion of Fe and Fe–Ni alloys

6.1. Linear thermal expansion coefficient (LTEC) of ferrite

The relative length-changes as a function of temperature of pure Fe and Fe–Ni alloys (Fe–2.96 at.%Ni and Fe–5.93 at.%Ni and) are shown in Figs. 9 and 11, respectively. The heat treatment cycles considered here (see Section 4.2.1) were carried out in normal mode. The magnetic transition temperature of Fe–2.96 at.%Ni was found to be 1033.3 ± 1 K, and the temperature calibration was performed as for pure Fe (see Section 4.3). For Fe–5.93 at.%Ni a value for the magnetic transition could not be obtained, because both during heating and cooling the magnetic transition appears in the temperature range of the $\alpha \rightarrow \gamma$ and the $\gamma \rightarrow \alpha$ transformation, respectively. Thus, for this alloy the temperature calibration was done on the basis of the magnetic transition measured separately for pure Fe (see Section 4.3).

Values for the linear thermal expansion, α (T), can be calculated from the relative length-change data according to

$$\alpha(T) = \frac{\mathrm{d}(\Delta L/L_0)}{\mathrm{d}T} \quad (5)$$

An analytical description for the temperature dependence of the relative length-change ($\Delta L/L_0$) of pure iron, ignoring the magnetic contribution to the thermal expansion of the ferrite and austenite phases, has been given in Ref. [11]. Recently, an analytical expression for the thermal expansion coefficient of ferrite, α_α was presented that does take into account both non-magnetic and magnetic contributions [7].

$$\alpha_\alpha = b + cT + \mathrm{d}T^2 + f_\mathrm{i} \exp(e_\mathrm{i} T^*)(T^*)^{g_\mathrm{i}}$$
$$300\,\mathrm{K} < T < 1185\,\mathrm{K} \quad (6)$$

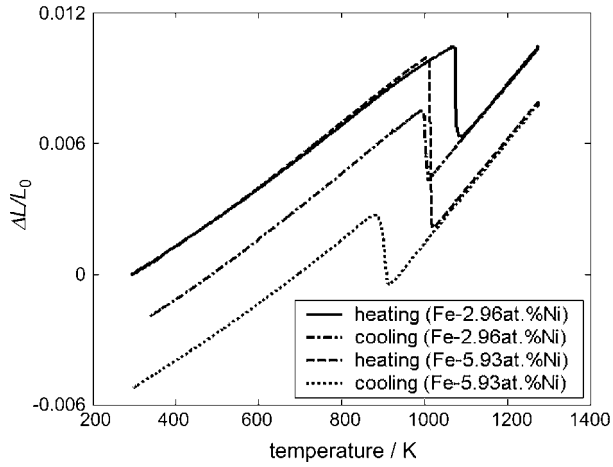

Fig. 11. Measured relative length-change as a function of temperature (T_{centre}), for two Fe–Ni alloys as indicated, during heating (20 K min^{-1}) from room temperature to 1273 K, with an intermediate isothermal annealing for 30 min, and during subsequent cooling (20 K min^{-1}) to room temperature.

where $T^* = |(T - T_C)/T_C|$, T_C denotes the Curie temperature, b to d are parameters representing the nonmagnetic contribution to α_α, and e_i to g_i are parameters that represent the magnetic contribution to α_α. The label i equals 1 if $T < T_C$, and equals 2 if $T > T_C$.

The thermal expansion coefficient of the ferrite phase of pure Fe as obtained by applying Eq. (5) to the relative length-change data given in Fig. 9, is shown in Fig. 12(a), along with the result obtained by fitting Eq. (6) to these α_α data. The thus obtained optimised LTEC data (values of b_α, $c_\alpha \cdots g_\alpha$; see Table 4) agree with corresponding values given in Ref. [7] within experimental accuracy; the small difference is due to the larger scatter in the measured LTEC data obtained with the present dilatometer with electromagnetic heating (DIL 805 A/D) as compared to the dilatometer with resistance heating (DIL 802).

Table 4
Values for the parameters in the analytical description (cf. Eq. (6)) of the thermal expansion of the ferrite phase of pure Fe, Fe–2.96Ni and Fe–5.93 at.%Ni, as obtained by fitting to the experimental data after length-change scale and temperature scale corrections as developed in this work

Alloys	Parameters	Parameter values
Pure Fe	b (K^{-1})	−4.61E−9
	c (K^{-1})	2.35E−8
	d (K^{-1})	−2.11E−11
	e_1	−1.30
	e_2	2.56
	f_1 (K^{-1})	1.57E−5
	f_2 (K^{-2})	1.45E−5
	g_1	0.04
	g_2	0.03
Fe–2.96 at.%Ni	b (K^{-1})	−4.22E−9
	c (K^{-1})	1.92E−8
	d (K^{-1})	−1.68E−11
	e_1	−1.15
	e_2	1.92
	f_1 (K^{-1})	1.39E−5
	f_2 (K^{-2})	1.19E−5
	g_1	0.07
	g_2	0.03
Fe–5.93 at.%Ni	b	1.08E−5
	c (K^{-1})	5.35E−9
	d (K^{-2})	2.25E−12

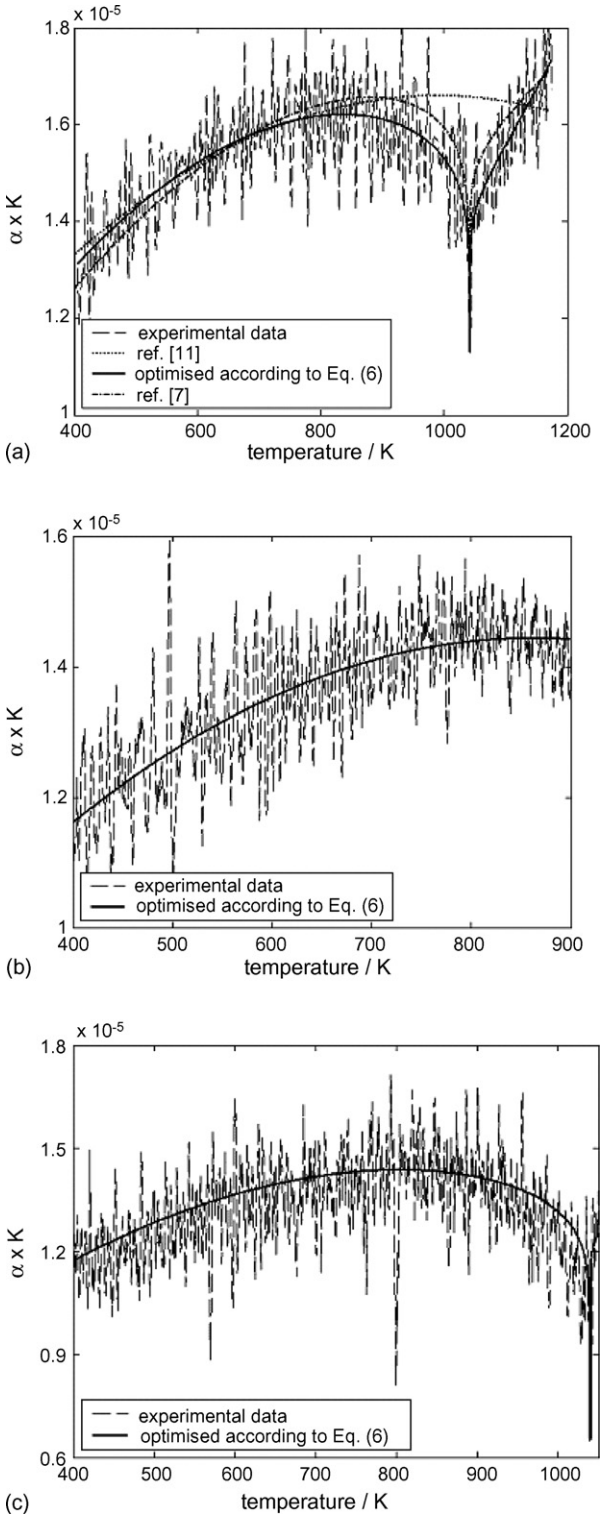

Fig. 12. Comparison of the measured (with a heating rate of 20 K min^{-1}), and optimized data according to Eq. (6) (full line) of ferritic (a) pure Fe, (b) Fe–5.93 at.%Ni, and (c) Fe–2.96 at.%Ni.

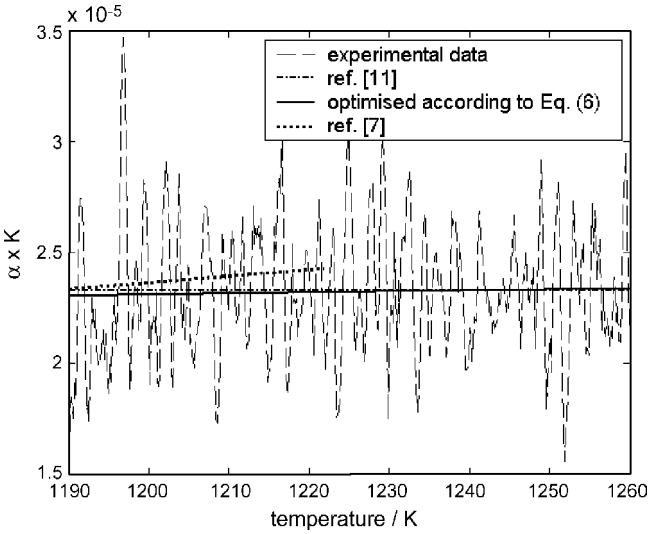

Fig. 13. Comparison of the measured and optimized data according to the linear terms in Eq. (6) (full line) of austenitic pure Fe.

The thermal expansion of the pure ferrite phase for Fe–5.93 at.%Ni is free from a magnetic transition and therefore only the non-magnetic contribution in Eq. (6) is fitted to the measured LTEC data of the ferritic Fe–5.93 at.%Ni. The thus obtained fit is shown in Fig. 12(b). For Fe–2.96 at.%Ni the magnetic transition occurs within the temperature range for thermal expansion of the single ferrite phase and hence the analytical expression given by Eq. (6), including magnetic and non-magnetic contributions, is fitted to the measured experimental LTEC data. The result is shown in Fig. 12(c). The obtained fit parameters for the LTEC of the ferrite phases of both Fe–5.93 at.%Ni and Fe–2.96 at.%Ni have been gathered in Table 4 as well.

6.2. Linear thermal expansion coefficient (LTEC) of austenite

An analytical description of the temperature dependence of the relative length-change of austenite by thermal expansion/shrinkage is given by the linear terms (first two terms: $b + cT$) of Eq. (6). By fitting this expression for LTEC of austenite upon cooling for both the pure Fe and Fe–Ni alloys, the linear thermal expansion coefficient of austenite has been obtained as:

$$\text{Fe} : 1.8 \times 10^{-5} + 4.6 \times 10^{-9} T, \qquad 1190\,\text{K} < T < 1260\,\text{K} \tag{7}$$

$$\text{Fe–2.96 at.\%Ni} : 2.1 \times 10^{-5} + 11.0 \times 10^{-10} T, \quad 1085\,\text{K} < T < 1260\,\text{K} \tag{8}$$

$$\text{Fe–5.93 at.\%Ni} : 2.1 \times 10^{-5} + 8.0 \times 10^{-10} T, \quad 1085\,\text{K} < T < 1260\,\text{K} \tag{9}$$

The LTEC for the austenite phase of pure Fe obtained in the present work agrees well with the data given in Ref. [11] (see Fig. 13). The corresponding data presented in Ref. [7] slightly deviate (see Fig. 13), which may be due to the small temperature range applied in Ref. [7].

7. Conclusions

1. Calibration of the temperature and length-change scales of a differential dilatometer is a prerequisite to accurately determine the (linear) thermal dilation as well the dilation associated with phase transitions. Corresponding corrections for a quenching and deformation differential dilatometer with an electromagnetic heating device have been developed for the normal, compressive and tensile loading modes.
2. The length-change calibration has to be performed for heating and cooling separately. The length-change calibration for the normal and compressive modes is possible applying a Pt reference specimen with known thermal dilation data and for the tensile mode applying pure iron as reference material.
3. The temperature calibration for both heating and cooling and for all modes can be performed utilizing the hysteresis-free Curie temperature of pure Fe.
4. Temperature calibration can be performed in situ if the investigated alloy exhibits a ferro-magnetic transition.
5. Although a quenching and deformation differential dilatometer with electromagnetic heating is naturally less accurate than a “normal” differential dilatometer with resistive heating, the LTEC obtained for the ferrite phase in the present work with the quenching and deformation dilatometer agrees well with the data obtained in Ref. [7] with a more accurate differential dilatometer.
6. The calibration correction methods developed in this work were applied successfully to determine the LTEC for both the ferrite phase and the austenite phase of Fe–2.96 at.%Ni and Fe–5.93 at.%Ni.

References

[1] E.J. Mittemeijer, J. Mater. Sci. 27 (1992) 3977.
[2] C. Capdevila, F.G. Caballero, C. Gracia de Andres, Metall. Mater. Trans. A 32 (2001) 66.
[3] C.M. Li, F. Sommer, E.J. Mittemeijer, Mater. Sci. Eng. A 325 (2002) 307.
[4] Y.C. Liu, F. Sommer, E.J. Mittemeijer, Acta Mater. 51 (2003) 507.
[5] H.K.D.H. Bhadeshia, Mater. Sci. Technol. 15 (1999) 22.
[6] G.H. Prior, Mater. Forum 18 (1994) 265.
[7] Y.C. Liu, F. Sommer, E.J. Mittemeijer, Thermochim. Acta 413 (2004) 215.
[8] G. Mohapatra, F. Sommer, E.J. Mittemeijer, Thermochim. Acta (2007), in press.
[9] Handbook of Thermophysical properties of Solid Materials, Ceramics, vol. 3, Pergamon Press, Oxford, 1961.
[10] A.T.W. Kempen, F. Sommer, E.J. Mittemeijer, Thermochim. Acta 383 (2002) 21.
[11] Y.S. Touloukian, Thermal Expansion: Metallic Elements and Alloys, Plenum Press, New York, 1975.
[12] A.T. Dinsdale, CALPHAD 15 (1991) 317.